Time-of-flight neutron diffraction and magnetization investigation of the crystal and magnetic structure of $YCo_{11}Ti$ and $YCo_{10}Mo_2$

Time-of-flight neutron diffraction and magnetization investigation of the crystal and magnetic structure of $YCo_{11}Ti$ and $YCo_{10}Mo_2$

O Moze†, L Pareti‡ and K H J Buschow§

† Dipartimento di Fisica, Università di Parma, Viale delle Scienze and Istituto Nazionale per la Fisica della Materia, Unità di Parma, Parma 43100, Italy
‡ Istituto Maspec del CNR, via Chiavari 18/a, Parma 43100, Italy
§ Van der Waals–Zeeman Laboratory, University of Amsterdam, Valckenierstrasse 65, 1018 XE Amsterdam, The Netherlands.

Abstract. The crystal and magnetic structures of the tetragonal compounds $YCo_{11}Ti$ and $YCo_{10}Mo_2$ (space group $I4/mmm$) have been investigated by time-of-flight neutron diffraction at 293 K. A strong site preference for both Ti and Mo atoms is observed, with these atoms almost exclusively occupying 8i sites. The refined Co moments at 8i, 8j and 8f sites are in agreement with magnetization measurements. The Co sublattice displays a uniaxial anisotropy for both compounds at room temperature. This is confirmed by bulk magnetization measurements using the SPD (singular point detection) technique. The compound $YCo_{11}Ti$ has been found to display a spin reorientation transition from axis to plane at approximately 650 K.

1. Introduction

The rare earth compounds of the type $RECo_{11}Ti$ and $RECo_{10}Mo_2$ belong to a large class of materials which crystallize in the tetragonal $ThMn_{12}$ ($I4/mmm$) structure. Both these compounds and those based on Fe have been regarded as potential starting materials for permanent magnet applications. Numerous x-ray and neutron diffraction investigations have revealed that there is a strong preference for the M atoms to occupy one of the three available sites 8i, 8j and 8f (figure 1) in $REFe_{12-x}M_x$ (M = Ti, V, Cr, Mo, Si and W) compounds [1]. Possible mechanisms for the observed preferential site occupancies have been presented in terms of atomic size effects as well as enthalpy considerations. Compounds with Co as a 3d component have been investigated but not as intensely as the corresponding Fe compounds.

Magnetization measurements performed on the systems $RECo_{11}Ti$ and $RECo_{10}Mo_2$ [2, 3] indicate that the 3d sublattice anisotropy gives rise to an easy magnetization direction along the tetragonal c-axis, as is also the case in Fe-based compounds of this structural type. For $RECo_{11}Ti$ compounds, the rare-earth sublattice anisotropy is governed by a positive second-order CEF parameter, $A_2^0 > 0$, and spin reorientation phenomena were observed for compounds with RE = Dy, Er and Tm. The average Co moment in this series at 4.2 K is approximately 1.4 μ_B. For $RECo_{10}Mo_2$ compounds, a much reduced Co moment results and a spin orientation has only been observed for $ErCo_{10}Mo_2$.

In this paper, the preferential site occupation and magnetic structure of $YCo_{11}Ti$ and $YCo_{10}Mo_2$ have been investigated by means of time-of-flight neutron powder diffraction in order to analyse the dependence of the Co sublattice magnetization on Ti and Mo
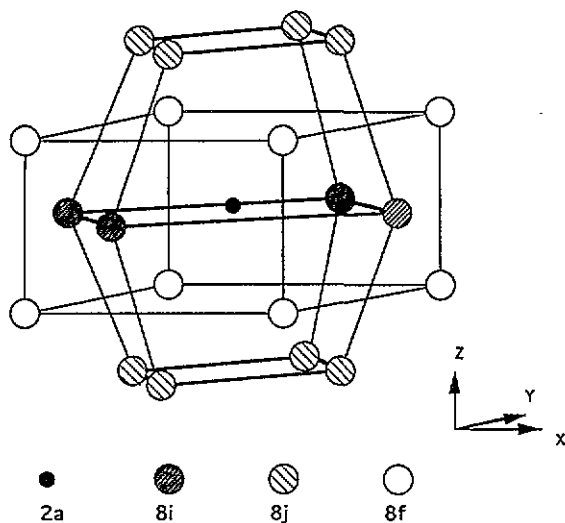
Figure 1. Plot displaying local co-ordination of transition metal atoms around the RE site of the ThMn$_{12}$ structure.

substitution. The former can easily be evidenced since there is a strong contrast in the neutron scattering lengths of (Co, Ti) and (Co, Mo) atoms. The relatively small neutron scattering length of Co means that observation of the magnetic scattering is more favourable in this case than with corresponding Fe compounds. Thus the Co moments at the three available sites have been refined, as has the direction of the Co sublattice magnetization. The singular point detection technique [4] has been used to measure the temperature dependence of the magnetic anisotropy field whilst thermomagnetic analysis was employed in order to determine the existence of magnetic phase transitions for both compounds between 293 and 1000 K. The refined Co magnetic moment magnitudes have been discussed in the light of recent electronic band structure calculations of these materials.

2. Experimental details

The samples used in the present investigation were prepared by arc-melting and subsequent annealing at 1050 °C for at least two weeks. Sample quality and homogeneity were verified by x-ray powder diffraction and thermomagnetic analysis. The samples were predominantly single-phase material, the diffraction lines showing the characteristics of the tetragonal ThMn$_{12}$ structure ($h + k + l = 2n$).

Neutron powder diffraction measurements were performed on the POLARIS high-intensity powder diffractometer at the ISIS neutron spallation source, Didcot, UK. Data were collected in two different configurations, one with a detector bank in backscattering $2\theta = 146°$ and the other in forward-scattering, $2\theta = 20°$. The instrumental resolution $\Delta d/d = 0.004$ ($d = $ lattice d-spacing) is constant for both the backscattering and the forward-scattering bank, but the resolution for the forward-scattering bank is a factor of four less. Diffraction data for both compounds were collected at 293 K. The data were normalized and corrected for absorption prior to use for refinement. Data collected in the backscattering mode allow for a particularly reliable decoupling of preferential occupation and thermal vibration parameters as quite small lattice d-spacings are accessed (down to

approximately 0.2 Å). For the forward-scattering bank, a total of 31 independent and overlapping reflections were used in the refinement whilst for the backscattering bank, 463 reflections were used. The magnetic anisotropy fields for both compounds were measured from 77 K to 293 K using the singular point detection (SPD) technique. Thermomagnetic analysis was also performed on both compounds from room temperature to 1100 K.

3. Results and analysis

The diffraction data collected on the diffractometer POLARIS were analysed by the Rietveld technique [5], using the program TF104M based on the Cambridge Crystallography Subroutine Library, CCSL [6] and developed for refinement of both crystal and magnetic structures. The appropriate neutron nuclear scattering lengths employed in the refinement were, respectively [7], $b_Y = 0.775 \times 10^{-12}$ cm, $b_{Co} = 0.249 \times 10^{-12}$ cm, $b_{Ti} = -0.343 \times 10^{-12}$ cm and $b_{Mo} = 0.6715 \times 10^{-12}$ cm. The following parameters were refined; a scale factor, peak profile and background function parameters, isotropic thermal vibration parameters for all sites, Co site populations for sites 8i, 8j and 8f and finally Co magnetic moments for these sites. A statistical distribution of Co atoms over the three sites was assumed prior to commencement of the refinement. The refinement strategy consisted of first fixing the Co moments on all sites to those obtained from bulk magnetization measurements, an average of 1.4 μ_B per Co atom for $YCo_{11}Ti$ and 1.0 μ_B per Co atom for $YCo_{10}Mo_2$, and refining step by step the structural parameters for data from the backscattering bank only. This was done for moments fixed to lie along the c-axis as well as in the basal plane. The highly anisotropic neutron spin–magnetic moment interaction allows the overall moment direction with respect to the unique axis to be determined even for powder materials with a configurational symmetry lower than cubic [8]. For a simple ferromagnet, with a single spin axis, the scattered intensity, for unpolarized neutrons, is proportional to the sum of the squares of the nuclear and magnetic structure factors

$$I = F_{nuc}^2 + \langle q_{hkl}^2 \rangle F_{mag}^2 \tag{1}$$

where $\langle q_{hkl}^2 \rangle$ is the average value of $\sin^2 \gamma$, with γ the angle between the moment direction and the scattering vector. This further simplifies to the following form;

$$\langle q_{hkl}^2 \rangle = 1 - \langle \cos^2 \gamma \rangle \tag{2}$$

with

$$\langle \cos^2 \gamma \rangle = \left[\tfrac{1}{2}(h^2 + k^2)a^{*2} \sin^2 \phi + l^2 c^{*2} \cos^2 \phi \right] d^2 \tag{3}$$

where ϕ is the angle between the moment direction and the c-axis, a^* and c^* reciprocal space lattice parameters and d is the lattice spacing for reflection (hkl). Thus, for tetragonal symmetry, the angle ϕ can be obtained. Of course, any possible moment direction in the a–b plane cannot be specified with powder data alone. The Co site moments were refined by fixing all the structural parameters obtained beforehand and subsequently refining only the Co moments at 8i, 8j and 8f sites for the forward-scattering bank data. This data set contains the first few peaks which have significant magnetic contributions, such as (110) and (200). The (200) peak in particular has a very small nuclear structure factor, and most of the intensity for this peak can be attributed to magnetic scattering. However, even the backscattering bank contained reflections which have strong magnetic contributions

and by which the moment direction and magnitude can also be properly specified from the expressions quoted above. In particular, the (301), (400), (321), (420), (411), (222), (440) and (602) peaks have large structure factors, and the calculated magnetic contribution to these is significant. This is due to the enhancement of the magnetic scattering since the nuclear scattering length for Co is relatively small. As a final step, all structural and magnetic parameters were refined simultaneously for moments oriented along the c-axis and in the basal plane for the backscattering bank data. This last step was warranted because of the large range in d-spacing which allows for the decoupling of thermal, occupational and magnetic moment parameters. Normally such a step leads to the occurrence of large correlation coefficients between the refined parameters. The only significant correlations (above 30%) were between individual background parameters (a total of 10 of these were refined), peak shape parameters (four of these were refined) and the thermal and occupation factors for site 8i (approximately 70%). However, separately refining the thermal and occupancy factors for this site did not change the overall Co occupancy for this site, which remained at approximately 75% for the Ti compound and 50% for the Mo compound. In any case, it is often unrealistic to assume a complete statistical independence between refined parameters. On the basis of the quoted expressions for the magnetic scattering, the residual R-factors for moments oriented in the basal plane were significantly higher than those for moments aligned along the c-axis (χ^2 of 3.8 for the planar structure versus a χ^2 of approximately unity for the axial structure for $YCo_{11}Ti$). This is convincing microscopic evidence for a uniaxial Co anisotropy in both systems. This is particularly evident for example for the (002) peak. For the uniaxial structure, this peak has a null magnetic structure factor, whilst for the planar structure, the calculated magnetic contribution is almost the same magnitude as the calculated nuclear contribution. In each case, the refined thermal and occupational parameters were, within the errors of the refinement, identical. For the planar structure, refined moments at sites 8i, 8j and 8f were 2.04(0.20), 1.14(0.15) and 1.12(0.20) μ_B respectively for $YCo_{11}Ti$. The observed and calculated diffraction pattern for $YCo_{11}Ti$ is displayed in figures 2(a) and 2(b) for the axial and planar configurations respectively. The conversion from neutron time-of-flight, TOF, to d-spacing (with d in Å) is TOF $= 6461.4d \sin\theta$, where 2θ is the angular position of the detector bank. The final refined structural and magnetic parameters for $YCo_{11}Ti$ and $YCo_{10}Mo_2$ are displayed in tables 1 and 2.

Table 1. The refined structural and magnetic parameters for $YCo_{11}Ti$ at 293 K with $a = 8.3674(3)$ Å and $c = 4.7108(1)$ Å; $R_{wp} = 3.0\%$, $R_{exp} = 3.38\%$, $(\chi^2) = R_{wp}/R_{exp} = 0.8$.

Atom	Site	x/a	y/a	z/c	B (Å²)	Co occupancy	μ_z (μ_B)
Y	2a	0	0	0	0.39(3)		
Co	8i	0.3512(3)	0	0	0.25(3)	0.76(2)	1.66(15)
Co	8j	0.2797(3)	1/2	0	0.39	1.00(1)	1.42(15)
Co	8f	1/4	1/4	1/4	0.32	1.00(1)	1.47(15)

The thermomagnetic curve for $YCo_{11}Ti$ is displayed in figure 3. The Curie points obtained from thermomagnetic analysis correspond to 750 K for $YCo_{11}Ti$ and 468 K for $YCo_{10}Mo_2$. For $YCo_{11}Ti$ there is a broad peak present, centred at approximately 650 K, which indicates a possible magnetic phase transition. This is better evidenced in figure 4 where the temperature dependence of the magnetic anisotropy field is displayed as a function of the reduced temperature T/T_c for both compounds. Quite clearly, for the compound $YCo_{11}Ti$, the magnetic anisotropy constant $K_1 = \frac{1}{2}H_aM_s$, where H_a is the anisotropy field
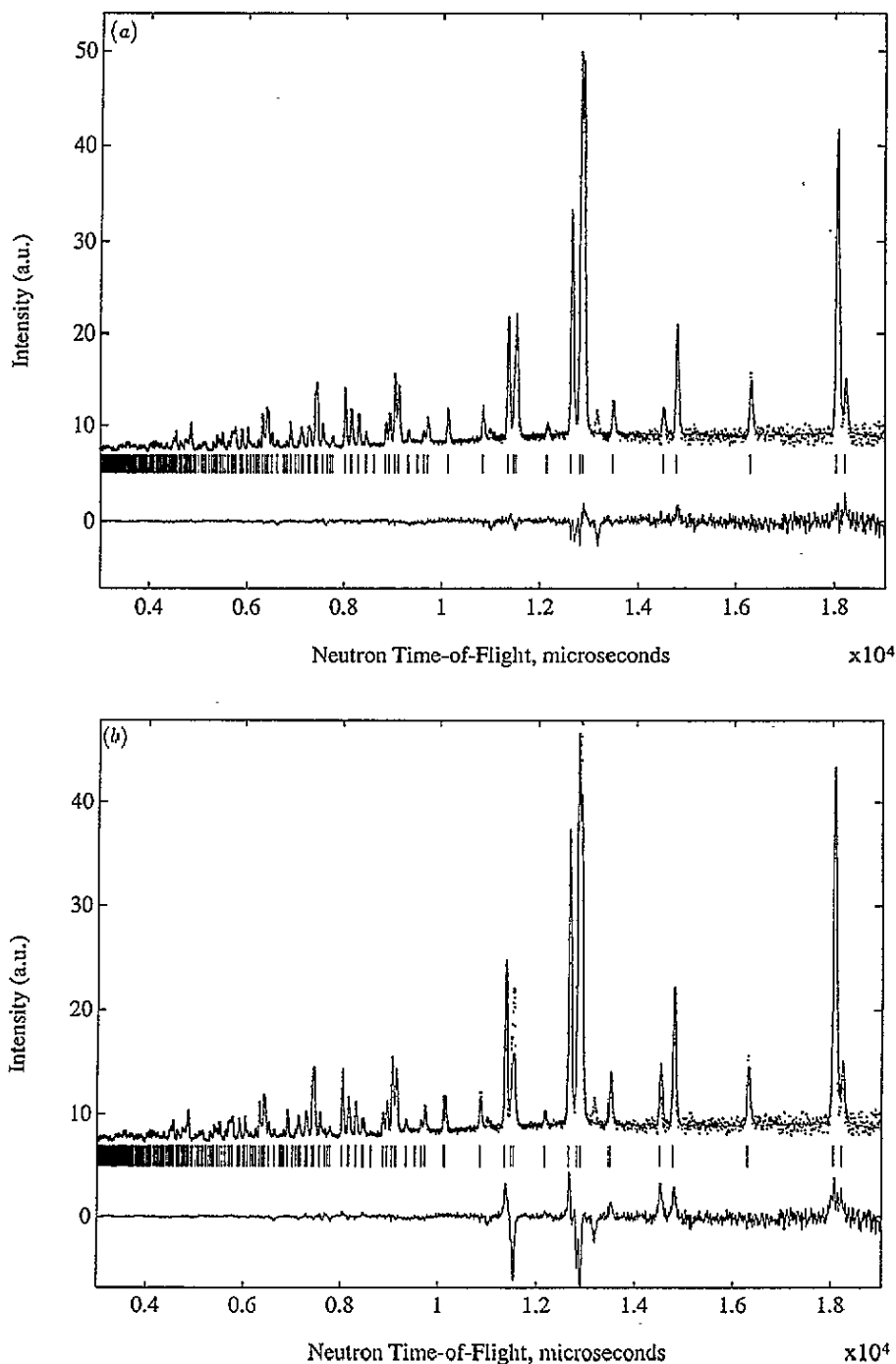
Figure 2. (a) The observed, calculated and difference neutron time-of-flight diffraction pattern for $YCo_{11}Ti$ at 293 K for Co moments lying along the tetragonal c-axis. The vertical bars indicate the calculated peak positions. Data displayed are for the backscattering bank at $2\theta = 145°$. (b) The observed, calculated and difference neutron time-of-flight diffraction pattern for $YCo_{11}Ti$ at 293 K for Co moments lying in the basal plane. The vertical bars indicate the calculated peak positions. Data displayed are for the backscattering bank at $2\theta = 145°$.

Table 2. Refined structural and magnetic parameters for $YCo_{10}Mo_2$ at 293 K with $a = 8.4301(3)$ Å and $c = 4.7211(1)$ Å; $R_{wp} = 1.2\%$, $R_{exp} = 0.62\%$, $(\chi^2) = R_{wp}/R_{exp} = 3.6$.

Atom	Site	x/a	y/a	z/c	B (Å^2)	Co occupancy	μ_z (μ_B)
Y	2a	0	0	0	0.46(3)		
Co	8i	0.3588(2)	0	0	0.37(3)	0.50(2)	0.81(20)
Co	8j	0.2814(2)	1/2	0	0.29	1.00(1)	0.52(20)
Co	8f	1/4	1/4	1/4	0.29	1.00(1)	0.71(20)

and M_s the saturation magnetization, appears to change sign well below the Curie point. This is evidence for a spin reorientation from axis to easy plane or easy cone. No such transition was observed for $YCo_{10}Mo_2$, which remains axial at all temperatures.

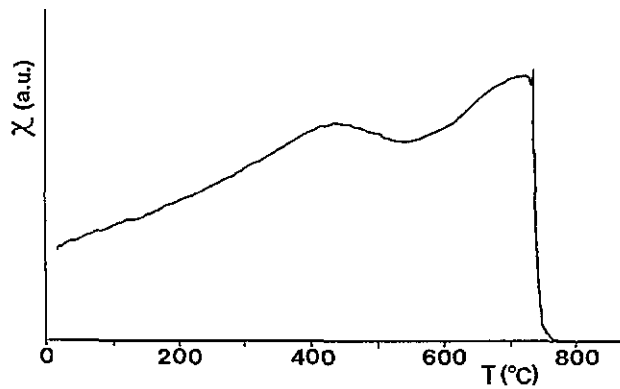**Figure 3.** The thermomagnetic analysis curve for $YCo_{11}Ti$.

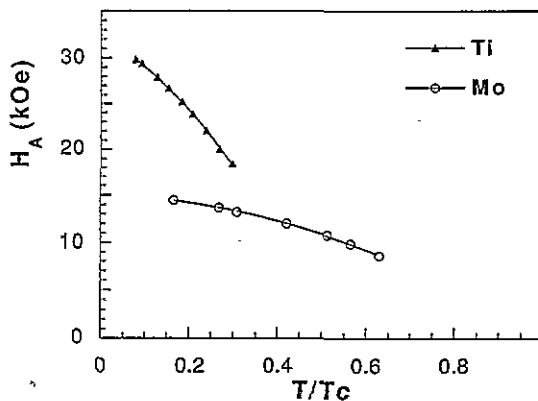**Figure 4.** The temperature dependence of the magnetic anisotropy field for $YCo_{11}Ti$ and $YCo_{10}Mo_2$.

4. Discussion

The result concerning the preferential site occupation confirms similar conclusions reached in previous diffraction investigations of the preferential site occupancy of M atoms in both $YFe_{12-x}M_x$ and $YCo_{12-x}M_x$ compounds. Metallic size and enthalpy considerations can in large part account for the observed preferential occupancy of Ti in $YFe_{11}Ti$ [9], V in $YFe_{10}V_2$ and $YCo_{10}V_2$ [10, 11], Si in $YNi_{10}Si_2$ [12], Mo in $NdFe_{10}Mo_2$ [13] and Cr in $YFe_{10}Cr_2$ [14] compounds.

The observed site dependence of the Co magnetic moments at the 8i, 8j and 8f sites follows the general trend observed for compounds of this structure type [1]. Given the observed occupation of Ti and Mo atoms at the 8i site, this site has the greatest number of Co first-nearest neighbours and largest average Co–Co distances but with, however, only one close Co neighbour; this results in an increased 3d density of states. The shortest Co–Co distances are those for 8f sites. These have the same number of Co nearest neighbours at 8j sites. Atoms at 8j and 8f sites have a higher close co-ordination of Co neighbours, giving rise to a reduced 3d density of states. The overall associated errors on the refined Co moments are significant, in particular for $YCo_{10}Mo_2$, but nevertheless the general trend also follows the predictions of site moments according to spin polarized band structure calculations [15, 16, 17]. The refined moments for both compounds are in good agreement with bulk magnetization measurements which give 14.2 μ_B per formula unit for $YCo_{11}Ti$ at 5 K and 6.4 μ_B per formula unit for $YCo_{10}Mo_2$ at 293 K. The greatly reduced Co moment observed for $YCo_{10}Mo_2$ could be accounted for by a Mo moment coupled antiferromagnetically with Co but this must await more detailed spin polarized band structure calculations and examination with polarized neutrons. However, since Mo is distributed only over the 8i site, even if this were the case, there still must be a significant reduction in Co moments at 8i and 8j sites in order to account for the overall reduction in saturation magnetization. Ohashi *et al* first correctly assigned axial anisotropy for Co in $YCo_{11}Ti$ [18] at the same time as Cheng *et al* [21]. The present neutron diffraction results resolve previous conflicting results [11, 19, 20, 21]. The observed axial anisotropy at room temperature of Co for this structure type is a peculiar trend given that Fe also displays an axial anisotropy. Up until now it has been generally observed that Fe and Co anisotropies are opposite (axial versus planar) in rare-earth intermetallic compounds [22, 23, 24]. The observed spin reorientation transition in $YCo_{11}Ti$ is a strong indication of the competing anisotropies between the three Co sublattices. Thus the occurrence of opposite contributions for Fe and Co can still be valid for the individual sites but the overall balance gives rise to the same sign of the anisotropy for both Fe and Co at room temperature.

References

[1] Li H S and Coey J M D 1991 *Handbook of Magnetic Materials* vol 6 (Amsterdam: North-Holland) pp 1–70

[2]   Brabers J H V J, Zeng D C, Tang N, de Boer F R and Buschow K H J 1995 *J. Magn. Magn. Mater.* **140–144** 1087

[3]   Zeng D C, Tang N, Zhao Z G, Buschow K H J and de Boer F R 1995 *J. Appl. Phys.* at press; 1988 *J. Less-Common Met.* **136** 207

[4]   Asti G and Rinaldi S 1972 *Phys. Rev. Lett.* **28** 1584

[5]   Rietveld H M 1969 *J. Appl. Crystallogr.* **2** 65

[6]   Brown J and Forsyth J B 1995 private communication

[7]   Sears V F 1992 *Neutron Scattering Lengths and Cross-Sections Neutron News* vol 3 (Reading: Gordon and Breach) p 26

[8]   Shirane G 1959 *Acta Crystallogr.* **12** 282

[9]   Moze O, Pareti L, Solzi M and David W I F 1988 *Solid State Commun.* **66** 465

[10] Moze O, Ibberson R M and Buschow K H J 1992 *J. Less-Common Met.* **70** 5986

[11] Solzi M, Pareti L, Moze O and David W I F 1988 *J. Appl. Phys.* **64** 5084

[12] Moze O, Ibberson R M and Buschow K H J 1991 *Solid State Commun.* **78** 473

[13] de Mooij D B and Buschow K H J 1988 *J. Less-Common Met.* **135** 207

[14] Moze O and Buschow K H J 1995 *J. Magn. Magn. Mater.* to appear

[15] Coehoorn R 1988 *J. Physique Coll.* **49** C8 301

[16] Coehoorn R 1990 *Phys. Rev.* B **41** 11 790

[17] Jaswal S S, Ren Y G and Sellmyer D J 1990 *J. Appl. Phys.* **67** 4564

[18] Ohashi K, Ido H, Honno K and Yoneda Y 1991 *Phys. Rev.* **70** 5986

[19] Solzi M, Xue R H and Pareti L 1990 *J. Magn. Magn. Mater.* **88** 44

[20] Yang Y, Kong L, Sun H, Yang J, Ding Y, Zhang B, Ye C and Jin L 1990 *J. Appl. Phys.* **67** 4632

[21] Cheng S F, Sinha V K, Ma B M, Sankar S G and Wallace W E 1991 *J. Appl. Phys.* **69** 5605

[22] Thuy N P, Franse J J M, Hong N M and Hien T D 1988 *J. Physique Coll.* C8 499

[23] Paoluzi A, Pareti L, Solzi T and Albertini F 1994 *J. Magn. Magn. Mater.* **132** 185

[24] Pareti L, Solzi M and Paoluzi A 1993 *J. Appl. Phys.* **73** 2941